

Hydrothermal synthesis of highly dispersed Bi–Ni–Sb–O pyrochlore for catalytic oxidation of carbon monoxide

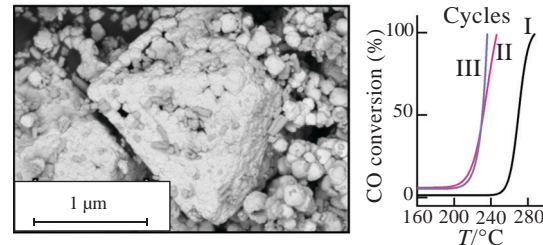
Anna V. Egorysheva,^{*a} Karina R. Plukchi,^a Svetlana V. Golodukhina,^a
Elena Yu. Liberman^b and Olga G. Ellert^a

^a *N. S. Kurnakov Institute of General and Inorganic Chemistry, Russian Academy of Sciences, 119991 Moscow, Russian Federation. E-mail: anna_egorysheva@rambler.ru*

^b *D. I. Mendeleev University of Chemical Technology of Russia, 125047 Moscow, Russian Federation*

DOI: 10.1016/j.mencom.2023.09.005

The highly dispersed Bi–Ni–Sb–O pyrochlore was prepared under hydrothermal conditions with and without microwave treatment. Composite samples of NiO/(Bi–Ni–Sb–O pyrochlore) demonstrated consistently high activity without pretreatment in CO oxidation.



Keywords: pyrochlore, Ni oxide, hydrothermal synthesis, morphology, catalysis, CO oxidation.

The catalytic oxidation of carbon monoxide is used to reduce its concentration in the atmosphere. Due to their ability to low-temperature CO oxidation, nickel-containing catalysts, which are cheaper than platinoids, are of particular interest.^{1–4} Their main disadvantage is rapid deactivation as a result of blocking the catalytic centers with carbon, a product of CO dissociation.^{2–7} This effect can be neutralized using composite materials consisting of Ni-containing particles applied onto an active support, characterized by the ability to redox transformations and high vacancy capacity providing a high mobility of oxygen.⁴ Complex antimonates possess these properties.^{8–11} In particular, iron- or cobalt-containing antimonates with the structures of pyrochlore and rosiaite are effective catalysts for CO oxidation and active Pd supports in methane oxidation.^{8,9,12,13} In this paper, we report the synthesis of highly dispersed Bi–Ni–Sb–O pyrochlore and data on the catalytic oxidation of CO with this pyrochlore used as a catalyst or an active NiO support.

The Bi₂O₃–NiO–Sb₂O₅ system has a region of solid solutions with a pyrochlore structure (Bi_{2-x}Ni_x)Ni_{2/3-y}Sb_{4/3+y}O_{7±δ}, x = 0.1–0.35, y = 0–0.1.¹⁴ Previously, this compound was obtained by a solid-phase reaction. However, a small specific surface area of the samples did not allow us to evaluate their catalytic properties. The highly dispersed powders were synthesized using a hydrothermal (HT) method. In order to optimize synthesis parameters under HT conditions, we investigated the dependence of the phase composition and morphology of samples on the precipitator concentration and the duration of synthesis.[†] We

[†] Bi(NO₃)₃·5H₂O (0.2182 g, 0.49 mmol) and Ni(NO₃)₂·6H₂O (0.063 g, 0.22 mmol) were dissolved in 10 ml of concentrated nitric acid, and this solution was added dropwise into a solution of Sb₂O₃ (0.0486 g, 0.33 mmol) in 30 ml of 4–9 M NaOH. The weights were calculated based on Bi_{1.8}Ni_{0.87}Sb_{1.33}O₇. The precipitate was kept for 30 min with stirring. The HT treatment of the suspension was carried out in 100 ml Teflon autoclaves (40% filling) at 200 °C for 48 and 80 h. The reaction products were washed and dried in air at 50 °C.

synthesized single-phase samples of Bi–Ni–Sb–O pyrochlore using a 6 M NaOH solution (Figure S1 in Online Supplementary Materials) because a concentration of 4–5 M was insufficient for precipitation, and a portion of Ni²⁺ and Bi³⁺ ions remained in the solution. In the precipitates obtained with a 7 M solution, a lack of antimony was observed due to its dissolution in a highly alkaline medium.

The formation of the Bi–Ni–Sb–O pyrochlore was recorded after HT treatment with 6 M NaOH solutions at 200 °C for 48 h (Figure S1). Due to an incomplete reaction, Ni(OH)₂ and δ-Bi₂O₃ impurities were also detected. A single-phase pyrochlore sample was obtained at a synthesis duration of 80 h [Figure 1(a)].[‡] The elemental composition of this sample was close to the theoretical one (Table S1). The coherent scattering regions (CSRs) of the Bi–Ni–Sb–O pyrochlores synthesized for 48 and 80 h were 28–30 nm. The samples obtained under HT processing for 80 h consisted of spherical particles of 100–150 nm, which were partially aggregated to form hollow octahedra with an edge length of 1–2 μm [Figure 1(b)].[§] The synthesis temperature of 190 °C

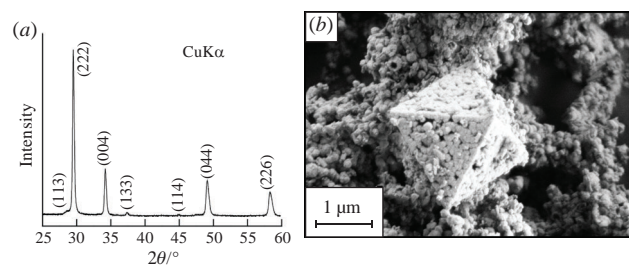


Figure 1 (a) X-ray diffraction pattern and (b) SEM image of Bi–Ni–Sb–O pyrochlores synthesized from the precursors precipitated with 6 M NaOH solution under HT conditions for 80 h at 200 °C.

[‡] X-ray diffraction patterns were obtained using a Bruker D8 Advance diffractometer (CuKα radiation, Ni filter, LYNXEYE detector).

[§] The morphology and elemental composition were studied using a Carl Zeiss NVision 40 three-beam workstation with the EDX function.

Table 1 Phase composition of the MWHT synthesis products.^a

Synthesis duration	NaOH solution molarity				
	5.5 M	6 M	7 M	8 M	9 M
1 h	$\delta\text{-Bi}_2\text{O}_3 + \text{P} + \beta\text{-Ni(OH)}_2 + \text{a.ph.}$	$\delta\text{-Bi}_2\text{O}_3 + \text{P} + \beta\text{-Ni(OH)}_2 + \text{a.ph.}$	$\text{F} + \text{P} + \delta\text{-Bi}_2\text{O}_3 + \beta\text{-Ni(OH)}_2 + \text{a.ph.}$	$\text{F} + \beta\text{-Ni(OH)}_2 + \text{a.ph.}$	$\beta\text{-Ni(OH)}_2 + \text{F} + \text{a.ph.}$
2 h	$\text{P} + \delta\text{-Bi}_2\text{O}_3 + \text{a.ph.}$	$\text{P} + \delta\text{-Bi}_2\text{O}_3 + \text{a.ph.}$	$\text{F} + \text{P} + \delta\text{-Bi}_2\text{O}_3$	F	F
3 h	$\text{P} + \delta\text{-Bi}_2\text{O}_3$	P	$\text{F} + \text{P}$	F	F

^a P, a pyrochlore phase; F, a fluorite-like phase; and a.ph., an amorphous phase. The phases are listed in a descending order of their concentrations.

(6 M NaOH) gave rise to the formation of $\beta\text{-Ni(OH)}_2$. Depletion of the B–N–S–O pyrochlore with nickel (Table S1) did not cause the appearance of a $\delta\text{-Bi}_2\text{O}_3$ impurity because of the existence of a solid solution $(\text{Bi}_{2x}\text{Ni}_x)\text{Ni}_{2/3-y}\text{Sb}_{4/3+y}\text{O}_{7 \pm \delta}$ with the pyrochlore structure.¹⁴

The advantages of microwave hydrothermal (MWHT) synthesis include the uniform heating of the entire reaction volume, which provides phase and morphological uniformity of the product, and a high rate of reaction. The HT synthesis was adapted to the conditions of MWHT treatment.¹¹ When a 5.5 M NaOH solution was used, trace amounts of $\delta\text{-Bi}_2\text{O}_3$ [Figure S2(a)] were detected along with pyrochlore in the reaction product, but in the case of 6 M NaOH, a single-phase B–N–S–O pyrochlore sample was obtained upon MWHT treatment at 220 °C for 3 h (Table 1). An alkali concentration of 7 M or higher gave rise to the appearance of a fluorite-like impurity phase, the concentration of which increased with molarity. The pyrochlore was not formed at an alkali concentration of >8 M. Thus, the use of MWHT processing makes it possible to reduce significantly the synthesis time.

Using XRD, SEM, and EDX analysis, we studied the sequence of phase transformations during the synthesis. All samples before MWHT treatment were X-ray amorphous [Figure S2(b)]. After 10 min of the treatment, the sample obtained using a 6 M NaOH solution consisted of crystalline intermediate products, which contained octahedral particles of a $\delta\text{-Bi}_2\text{O}_3$ solid solution (approximate composition, $\text{Bi}_{1.5}\text{Sb}_{0.5}\text{O}_3$), large spherical particles (2–5 μm) of a fluorite-like phase of $10\text{NiO}-25\text{Sb}_2\text{O}_5-65\text{Bi}_2\text{O}_3$, and thin nanocrystalline $\beta\text{-Ni(OH)}_2$ plates (Figure 2). After 30 min, small spherical particles crystallized on the surface of octahedral $\delta\text{-Bi}_2\text{O}_3$ crystals, the composition of which was close to the $\text{Bi}_{1.8}\text{Ni}_{0.87}\text{Sb}_{1.33}\text{O}_7$ pyrochlore. At a synthesis duration of 1 h, the entire $\delta\text{-Bi}_2\text{O}_3$ surface was covered with a layer of octahedrally aggregated pyrochlore particles. In the process of synthesis, a $\delta\text{-Bi}_2\text{O}_3$ solid solution gradually dissolved to result in a hollow pyrochlore octahedron. Large particles of the fluorite-like phase and nickel hydroxide plates also dissolved. Therefore, after 2 h of MWHT treatment, the sample consisted of individual pyrochlore particles, octahedral aggregates formed from them, and an insignificant amount of unreacted components.

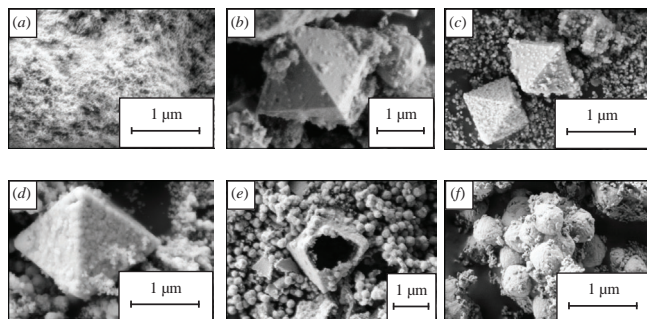


Figure 2 SEM images of the samples prepared using 6 M NaOH (a) before and after the MWHT treatment for (b) 10 min, (c) 30 min, (d) 1 h, (e) 2 h, and (f) 3 h.

[†] Synthesis was carried out using a Milestone Ethos Up system.

Further growth of spherical pyrochlore particles resulted in the destruction of octahedral aggregates, and only spherical particles were observed after 3 h of MWHT treatment. In the sample obtained in a 7 M alkaline solution, the fluorite-like phase did not dissolve. Its composition gradually changes to $4\text{NiO}-20\text{Sb}_2\text{O}_5-76\text{Bi}_2\text{O}_3$, and the synthesized sample was a mixture of the Bi–Ni–Sb–O pyrochlore and the fluorite-like phase. At a higher alkali concentration, the $\delta\text{-Bi}_2\text{O}_3$ solid solution was not formed, and the synthesis resulted in a single-phase fluorite-like sample.

A comparison of the activity of Bi–Ni–Sb–O pyrochlore samples obtained under HT and MWHT conditions revealed no difference in their catalytic properties in the CO oxidation reaction.^{††} Both samples demonstrated activity in CO oxidation, decreasing with repeated heating cycles in the flow of a CO + O₂ model gas mixture (Table 2, Figure S3). The CSRs of the samples before and after the catalytic reaction were 32 and 29 nm, respectively, and they indicate the absence of particle sintering.

Significant differences were observed for the Bi–Ni–Sb–O pyrochlore sample with $\beta\text{-Ni(OH)}_2$ particles on the surface. The activity of this sample (6 M NaOH, HT, 190 °C, 80 h) increased after the first cycle and further did not change [Figure 3(a)]. It is well known that at above 260 °C, $\beta\text{-Ni(OH)}_2$ decomposes into NiO and H₂O.^{1,15} This process gave rise to the appearance of a catalytically active NiO phase and the disappearance of $\beta\text{-Ni(OH)}_2$ on the pyrochlore surface after the first heating cycle [Figure 3(b)]. It is most likely that NiO formed at low temperatures was present on the surface in a nanocrystalline or amorphous state, which cannot be detected in the XRD pattern. Note that the morphology of particles on the Bi–Ni–Sb–O pyrochlore surface upon the decomposition of $\beta\text{-Ni(OH)}_2$ remained unchanged. The rectangular nanocrystallites 50–100 nm long are clearly visible on the surface of the Bi–Ni–Sb–O pyrochlore particles before and after catalysis [Figures 3(c), (d)]. Thus, after the first heating cycle, the sample was a composite catalyst consisting of a Bi–Ni–Sb–O pyrochlore support and a NiO active component. Stability that is ensured by the promotional effect of the support is an advantageous difference

Table 2 Temperatures of 50 and 90% conversions in cycling tests over Bi–Ni–Sb–O pyrochlore synthesized under different conditions.

Cycle	Conversion temperature/°C					
	HT (200 °C) $S_{\text{BET}} = 4.6 \text{ m}^2 \text{ g}^{-1}$ ^a		MWHT (220 °C) $S_{\text{BET}} = 2.6 \text{ m}^2 \text{ g}^{-1}$		HT (190 °C), $S_{\text{BET}} = 6.5 \text{ m}^2 \text{ g}^{-1}$	
	50%	90%	50%	90%	50%	90%
I	329	437	298	345	270	280
II	402	490	336	415	230	243
III	-	-	367	438	230	235

^a Measured using low-temperature nitrogen adsorption on an ATX-06 analyzer (carrier gas, helium of grade A) according to the Brunauer–Emmett–Teller (BET) model.

^{††} The catalytic activity in CO oxidation was evaluated in a fixed bed quartz tube reactor with 0.2 g of a catalyst. Reagent gases (1.5 vol% CO, 10 vol% O₂, and the balance N₂) passed through the reactor at a rate of 100 ml min⁻¹. The outlet gas composition was controlled by gas chromatography.

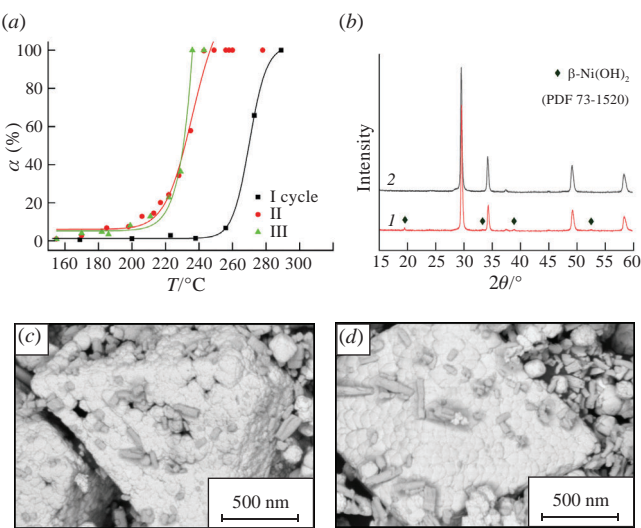


Figure 3 (a) Temperature dependences of CO conversion (α) on the Bi–Ni–Sb–O pyrochlore with β -Ni(OH)₂ particles on the surface, synthesized by HT (6 M NaOH, 190 °C, 80 h); (b) X-ray diffraction patterns and (c),(d) backscattered mode images of the sample 1 (c) before and 2 (d) after the first cycle of the catalytic test.

between this catalyst and simple NiO oxide.^{2–7} Another advantage of the NiO/(BiNiSb–O pyrochlore) catalysts is the formation of a NiO active component on the support surface as a result of β -Ni(OH)₂ decomposition in a reaction atmosphere of CO + O₂. Thus, we excluded the stage of impregnation to simplify the synthesis process.

Thus, we developed methods for the synthesis of highly dispersed single-phase Bi–Ni–Sb–O pyrochlore under hydrothermal and microwave hydrothermal conditions. The β -Ni(OH)₂/(Bi–Ni–Sb–O pyrochlore) composite was prepared by one-step synthesis. After decomposition of β -Ni(OH)₂ at >260 °C, this composite transformed into a NiO/(Bi–Ni–Sb–O pyrochlore) catalyst, which is stable and promising for use in the CO oxidation reaction.

This work was supported by the Russian Science Foundation (grant no. 23-23-00113).

Online Supplementary Materials

Supplementary data associated with this article can be found in the online version at doi: 10.1016/j.mencom.2023.09.005.

References

- 1 D. Wang, R. Xu, X. Wang and Y. Li, *Nanotechnology*, 2006, **17**, 979.
- 2 S. Royer and D. Duprez, *ChemCatChem*, 2011, **3**, 24.
- 3 J. Zhu and Q. Gao, *Microporous Mesoporous Mater.*, 2009, **124**, 144.
- 4 S. Mahammadunnisa, P. M. K. Reddy, N. Lingaiah and C. Subrahmanyam, *Catal. Sci. Technol.*, 2013, **3**, 730.
- 5 J. M. D. Tascón and L. González Tejeda, *React. Kinet. Catal. Lett.*, 1980, **15**, 185.
- 6 S. Dey and N. S. Mehta, *Chem. Eng. J. Adv.*, 2020, **1**, 100008.
- 7 S. Trivedi, R. Prasad and S. K. Gautam, *AIChE J.*, 2018, **64**, 2632.
- 8 O. G. Ellert, A. V. Egorysheva, E. Yu. Liberman, S. V. Golodukhina, D. I. Kirdyankin and O. M. Gajtko, *Inorg. Mater.*, 2019, **55**, 1257 (*Neorg. Mater.*, 2019, **55**, 1355).
- 9 O. G. Ellert, A. V. Egorysheva, E. Yu. Liberman, S. V. Golodukhina, O. V. Arapova and G. N. Bondarenko, *Ceram. Int.*, 2020, **46**, 27725.
- 10 M. M. Gadgil and S. K. Kulshreshtha, *J. Mol. Catal. A: Chem.*, 1995, **95**, 211.
- 11 S. R. G. Carrazán, L. Cadus, P. Dieu, P. Ruiz and B. Delmon, *Catal. Today*, 1996, **32**, 311.
- 12 A. V. Egorysheva, O. G. Ellert, E. Yu. Liberman, S. V. Golodukhina, O. V. Arapova, P. A. Chistyakova and A. V. Naumkin, *Russ. J. Inorg. Chem.*, 2022, **67**, 2127.
- 13 S. V. Golodukhina, L. S. Razvorotneva, A. V. Egorysheva, O. G. Ellert and V. K. Ivanov, *Dokl. Chem.*, 2021, **500**, 199 (*Dokl. Ross. Akad. Nauk, Khim., Nauki Mater.*, 2021, **500**, 29).
- 14 A. V. Egorysheva, O. G. Ellert, Y. V. Zubavichus, O. M. Gajtko, N. N. Efimov, R. D. Svetogorov and V. Yu. Murzin, *J. Solid State Chem.*, 2015, **225**, 97.
- 15 D.-B. Kuang, B.-X. Lei, Y.-P. Pan, X.-Y. Yu and C.-Y. Su, *J. Phys. Chem. C*, 2009, **113**, 5508.

Received: 27th March 2023; Com. 23/7133